RSC Advances

PAPER

Cite this: *RSC Adv.*, 2015, **5**, 33249

Uranium(VI) complexes with isonicotinic acid: from monomer to 2D polymer with unique U–N bonding†

Yingjie Zhang,*[a] Inna Karatchevtseva,[a] Jason R. Price,[b] Igor Aharonovich,[c] Fatima Kadi,[a] Gregory R. Lumpkin[a] and Feng Li[d]

Received 22nd January 2015
Accepted 2nd April 2015

DOI: 10.1039/c5ra01272d

www.rsc.org/advances

Two new uranium(VI) complexes with isonicotinic acid (HINT) have been synthesized and characterized. $[(UO_2)(NO_3)_2(HINT)_2]$ (**1**) has a monomeric structure constructed of a hexagonal bipyramidal uranyl centre, two nitrate anions and two monodentate HINT in *trans*-positions. $[(UO_2)(OH)(INT)]$ (**2**) has a two-dimensional (2D) polymeric structure constructed of uranyl hydroxyl 1D pillars and μ_3-bridging INT anions; the first observation of INT in μ_3-bridging mode for U(VI) ion *via* U–N bonding. Thermal analysis confirmed both complexes lost coordinated INT ligands followed by further decomposition to form U_3O_8. Raman spectroscopy has confirmed the presence of uranyl ion and INT ligand in both complexes as well as the existence of nitrate vibrations in **1** and hydroxyl vibrations in **2**. Their photoluminescence properties have been investigated.

Introduction

Metal–organic complexes and hybrid materials with transition metals and lanthanide ions have been extensively studied in the last fifteen years mainly due to their structural diversity and potential industrial applications.[1] Such work on uranium(VI) is also important due to its relevance to the nuclear fuel cycle and the potential impact on the environment. For example, uranyl [U(VI)] complexes are generally soluble and are the major species involved in the migration processes and the formation of U(VI) complexes with environmentally relevant organic ligands such as carboxylates[2] is likely to have an impact on the mobility of U(VI) species in the environment.[3] In addition, some U(VI) hybrid materials have unique structures and properties making them potential new functional materials.[4]

U(VI) complexes with isonicotinic acid (HINT) have been relatively less studied and the available structures include a 1D polymer with uranyl hydroxyl dimer as a building unit[5] and several mixed ligand complexes, *e.g.* a dimer with CrO_4^{-},[6] 1D polymers with F^- (ref. 7) and a polymer with oxalate.[8] In addition, some U(VI) complexes with other monocarboxylate ligands similar to HINT were also documented earlier, *e.g.* oxypyridine-4-carboxylic acid,[9] picolinic acid,[10] pyrazine-2-carboxylic acid and pyrimidine-2-carboxylic acid.[11] Two conclusions can be drawn from the literature survey on U(VI) complexes with pyridine-based carboxylate ligands. Firstly, monomeric structures are relatively less reported as the carboxylate group tends to form bridging mode linking uranyl centres together. Secondly, U–N bonds are only observed together with the nearby carboxylate group chelating to the same uranyl centre. In fact, no isolated U–N bonding has been reported for U(VI) ion with INT ligand. In this work, we aim to further explore and expand the structural chemistry of U(VI) with HINT and herein report the synthesis, spectroscopic and thermal studies, photoluminescence and crystal structures of two new compounds, $[(UO_2)(NO_3)_2(HINT)_2]$ (**1**) with a monomeric structure and $[(UO_2)(OH)(INT)]$ (**2**) with a 2D layered structure *via* a unique μ_3-coordination mode of INT through bridging carboxylate group and U–N bonding.

Experimental section

Synthesis

$[(UO_2)(NO_3)_2(HINT)_2]$ (**1**). 2.0 mmol of isonicotinic acid (0.246 g) was dissolved in 10 mL of deionised (DI) water. 2.0 mL of uranyl nitrate solution (0.5 M) was then added to the above solution. Yellow crystalline product of **1** (~0.48 g) was formed after three weeks, with yield of ~75%. $C_{12}H_{10}N_4O_{12}U$ (FW = 640.26): calc. C, 22.51; H, 1.57; N, 8.75; found: C, 22.32; H, 1.65; N, 8.64.

$[(UO_2)(OH)(INT)]$ (**2**). 2.0 mL of uranyl nitrate solution (0.5 M), 1.0 mmol of isonicotinic acid (0.123 g), 1.2 mmol of KOH (0.067 g) and 5.0 mL of DI water were added in a 30 mL

[a]*Australian Nuclear Science and Technology Organisation, Locked Bag 2001, Kirrawee DC, NSW 2232, Australia. E-mail: yingjie.zhang@ansto.gov.au*

[b]*Australian Synchrotron, 800 Blackburn Road, Clayton, VIC 3168, Australia*

[c]*School of Physics and Advanced Materials, University of Technology Sydney, Ultimo, New South Wales 2007, Australia*

[d]*School of Science and Health, University of Western Sydney, Locked Bag 1797, Penrith, NSW 2751, Australia*

† Electronic supplementary information (ESI) available: SEM-EDS, TG/DTA, Raman assignments. CCDC 1035178 and 1035179. For ESI and crystallographic data in CIF or other electronic format see DOI: 10.1039/c5ra01272d

sealed titanium pressure vessel and left in a 180 °C oven for 48 hours. Yellow crystalline product of **2** (~0.20 g) was formed after slow cooling (<5 °C h^{-1}) to room temperature in a light yellow solution ($pH_f \sim 5.4$) with ~48% yield. $C_6H_5NO_5U$ (FW = 409.14): calc. C, 17.61; H, 1.23; N, 3.42; found: C, 17.54; H, 1.28; N, 3.56.

Both complexes were further characterized by elemental analysis, scanning electron microscope-electron disperse spectroscopy (SEM-EDS), thermogravimetric and differential thermal analysis (TG/DTA), Raman spectroscopy, photoluminescence and single crystal X-ray diffraction. SEM-EDS confirmed the presence of C, N, O and U in both complexes (Fig. S1 and S2†).

Characterization

Elemental analyses were carried out using a Perkin-Elmer 2400 CHN elemental analyzer. SEM-EDS was conducted under an accelerating voltage of 20 kV with a Zeiss Ultra Plus SEM (Carl Zeiss NTS GmbH, Oberkochen, Germany). The Raman spectra were recorded on a Perkin Elmer Raman station 400 with Micro300 Microscope and excitation laser 785 nm in the range 2000–100 cm^{-1}. TG/DTA was made on a SEIKO 6300 Thermal Analyzer from room temperature to 1000 °C at a heating rate of 10 °C min^{-1} and an air flow rate of 300 cm^3 min^{-1}. Fluorescence emission spectra were measured using a Cary Eclipse Fluorescence Spectrometer.

X-ray diffraction

The single crystal X-ray diffraction measurements were carried out on the MX2 beamline at the Australian Synchrotron. Diffraction data were collected using Si<111> monochromated synchrotron X-ray radiation (λ = 0.72930) at 100 (2) K with BlueIce software[12] and were corrected for Lorentz and polarization effects using the XDS software.[13] The structures were solved by direct methods and the full-matrix least-squares refinements were carried out using SHELX suite of programmes.[14]

Results and discussion

Structure descriptions and discussion

The crystal data and refinement details for **1** and **2** are summarized in Table 1. The asymmetric unit of **1** contains half a uranyl ion, coordinated by a nitrate anion and a monodentate HINT. The expansion by symmetry suggests that **1** has a monomeric structure with a hexagonal bipyramidal uranyl ion coordinated by two nitrate groups and two HINT, in *trans*-positions (Fig. 1a and b). The uranyl group is ideally linear [O=U=O angle of 180.00(2)°] with the U=O bond length of 1.765 (3) Å. The U–O bond lengths in the equatorial plane of the uranyl ion range from 2.543(3) to 2.554(3) Å for nitrate anions and 2.311(3) Å for the carboxylate O atom from HINT ligands. A ball-stick packing view (Fig. 1c) shows how the monomers pack in the crystal lattice. The calculated inter-molecule hydrogen bonds are summarized in Table 2. Apart from strong hydrogen bonds between the terminal carboxylate oxygen atoms (O5) and

Table 1 Crystal data and refinement details for **1** and **2**

Complex	**1**	**2**
Formula	$C_{12}H_{10}N_4O_{12}U$	$C_6H_4NO_5U$
Formula weight	640.27	409.14
Crystal system	Monoclinic	Orthorhombic
Space group	*C*2/*c*	*Pbca*
a (Å)	14.539(3)	10.191(2)
b (Å)	9.16999(18)	8.6030(17)
c (Å)	13.700(3)	18.665(4)
β (°)	116.31(3)	90
Volume (Å^3)	1637.2(7)	1636.4(6)
Z	4	8
μ (mm^{-1})	4.648	9.108
Min./Max. θ [°]	2.787/28.278	2.239/24.993
d_{calcd} (g cm^{-3})	2.597	3.321
GOF	1.0543	1.107
Final $R_1{}^a$ [$I > 2\sigma(I)$]	0.0200	0.0305
Final $wR_2{}^b$ [$I > 2\sigma(I)$]	0.0573	0.0772

^{a} $R_1 = \Sigma||F_o| - |F_c||/|F_o|$. ^{b} $wR_2 = \{\Sigma[w(F_o{}^2 - F_c{}^2)^2]/\Sigma[w(F_o{}^2)^2]\}^{1/2}$.

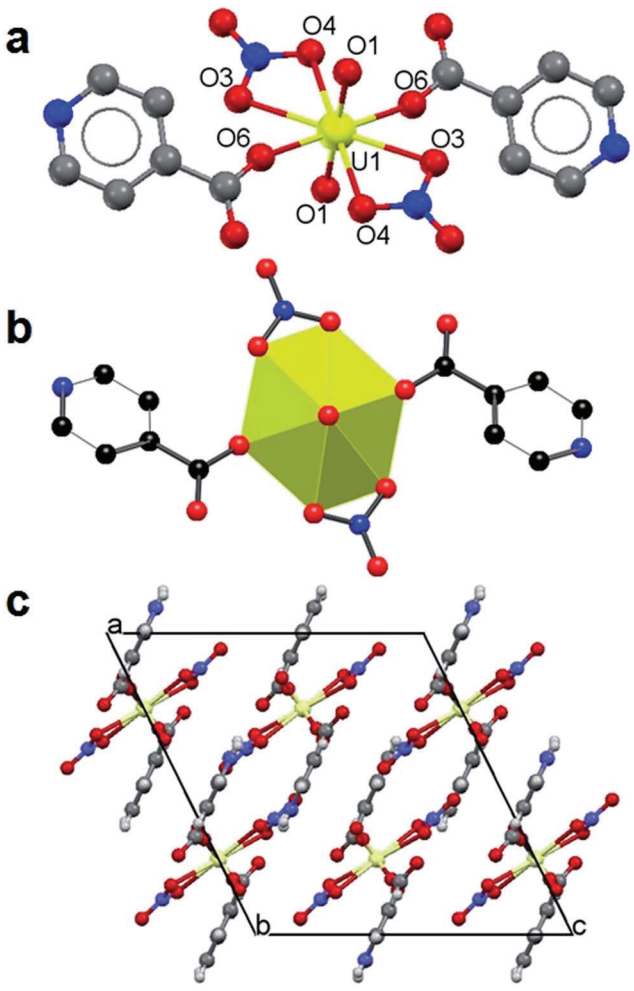

Fig. 1 Structure of **1**: ball-stick (a) and polyhedral (b) views of the monomeric structure and a packing view along the crystallographic *b*-axis (c).

Table 2 Calculated potential hydrogen bonds in **1** and **2**

Donor	H	Acceptor	D–H	H···A	D···A	D–H···A
Complex 1						
N2	H2	O5	0.71	2.11	2.71	144
C3	H3	O1	0.93	2.56	3.20	127
C4	H4	O2	0.93	2.34	3.25	167
C5	H5	O4	0.93	2.59	3.23	126
C6	H6	O2	0.93	2.42	3.32	161
Complex 2						
O3	H3	O2	0.85	2.11	2.94	165
C4	H4	O1	0.93	2.38	3.13	138
C5	H5	O1	0.93	2.46	3.30	150

the nitrogen atoms (N2) of the pyridine rings, uranyl oxygen atoms (O1) and majority of the nitrate oxygen atoms (O2 and O4) are involved in weak hydrogen bonding with the C–H from the pyridine rings leading the monomeric structure into three dimensions. Such neutral uranyl nitrate complexes with monodentate O-donor ligands in *trans*-arrangement are common[15] and the closely related one is the uranyl nitrate complex with pyridine-3-carboxylic acid.[16]

Complex **2** has a 2D polymeric structure built with pentagonal bipyramidal uranyl centres (Fig. 2a and b) *via* corner-sharing hydroxyl groups forming 1D uranyl hydroxyl pillars (Fig. 2c) which are further linked through μ_3-bridging INT anions to form the 2D layered structure (Fig. 2d) with layers closely packed in the crystal lattice (Fig. 2e). The uranyl unit is normal with O=U=O angle of 178.57(2)° and U=O bond lengths of 1.782(2) and 1.787(4) Å. The U–O bond lengths in the equatorial plane range from 2.316(4) to 2.379(4) Å for hydroxyl oxygen atoms (O_{-OH}) and 2.360(4) to 2.436(4) Å for O_{-COO} atoms. The N atom of the pyridine-ring occupies the fifth coordination position with U–N bond length of 2.574(5) Å. Inter-molecule hydrogen bonds (Table 2) include strong interactions between O_{-yl} (O2) and O_{-OH} (O3) groups and weak interactions between O_{-yl} (O1) and C–H (C4 and C5) leading the 2D structure into three dimensions.

A uranyl hydroxyl complex with INT anion was previously reported.[5] It has a 1D polymeric structure constructed with the uranyl hydroxyl dimer as the building unit and μ_2-bridging INT anions. In contrast, complex **2** has a 2D layered structure constructed with uranyl hydroxyl 1D pillars linked through μ_3-bridging INT anions. It is believed that the relatively higher final solution pH (~5.4) and consequently further hydrolysis of uranyl species lead to the formation of complex **2** with 1D uranyl hydrolysis pillars. In addition, it is rare to observe INT in μ_3-bridging mode for actinide ions and such coordination mode of INT was only found in a Np(v) complex before.[17]

Thermal stability

The DTA curve of **1** (Fig. S3†) has a small endotherm at ~275 °C and a large exotherm at ~450 °C with obvious three continuous decomposition steps. The first two steps from ~250 to ~420 °C with a weight loss of ~38% correspond to the decomposition of

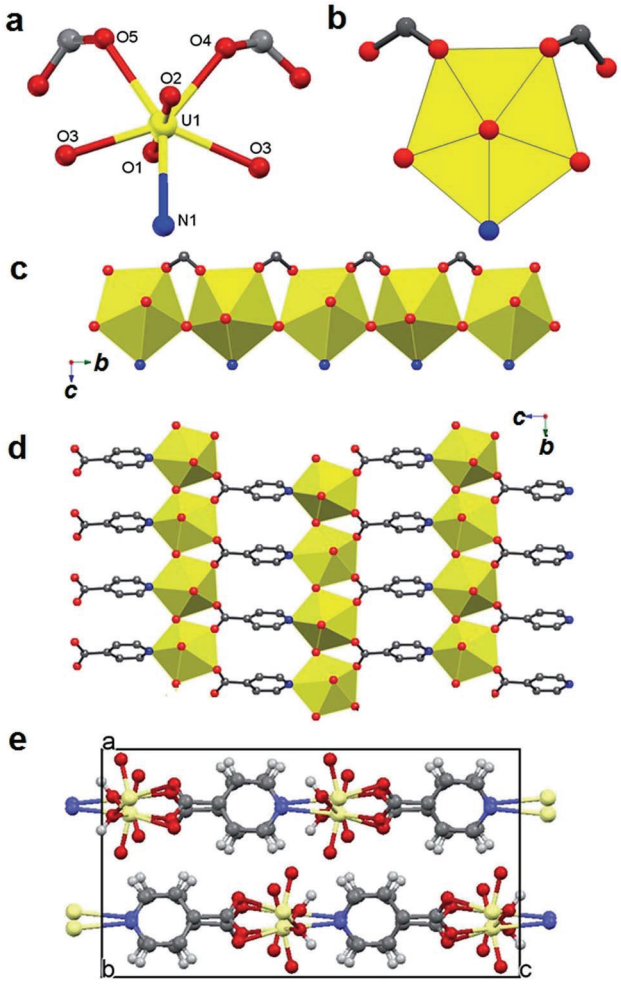

Fig. 2 Structure of **2**: ball-stick (a) and polyhedral (b) views of the pentagonal bipyramidal uranyl unit, a 1D uranyl hydroxyl pillar (c) formed by corner-sharing hydroxyl groups, a 2D layer (d) formed *via* μ_3-bridging INT ligands and a packing view along the crystallographic *b*-axis (e).

HINT ligands (calc. 38.4%) and the last step at ~450 °C is due to the decomposition of nitrate anions with the final product of U_3O_8 (residue: calc. 43.8%; found 44.7%). Similarly, the large exotherm at ~410 °C for **2** (Fig. S3†) corresponds to the decomposition of INT ligand with the final product of U_3O_8 (residue: calc. 68.6%; found 68.1%). Note uranium oxide phase transitions at high temperature in air have been well documented.[18] β-UO_3 is first formed at temperatures around 425 to 450 °C, which transforms to γ-UO_3 at ~500 °C. Further phase transition from γ-UO_3 to U_3O_8 occurs at 650 to 710 °C. Consequently, U_3O_8 is the main oxide phase present after heating to over 710 °C, which has been confirmed previously by both DSC/TG and powder X-ray diffraction studies.[18]

Raman spectroscopy

Raman spectroscopic characterization of both **1** and **2** (Fig. 3) confirmed: (1) the presence of uranyl groups in **1** and **2** with ν_s $(UO_2)^{2+}$ at 828 and 833 cm^{-1}, corresponding to the calculated

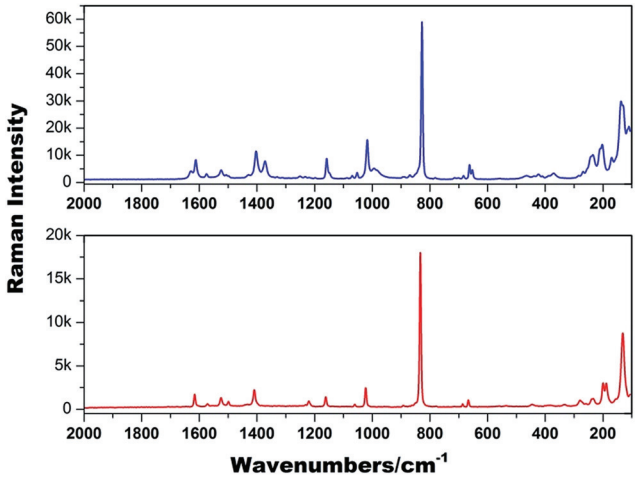

Fig. 3 Raman spectra (2000–100 cm^{-1}) of **1** (top) and **2** (bottom).

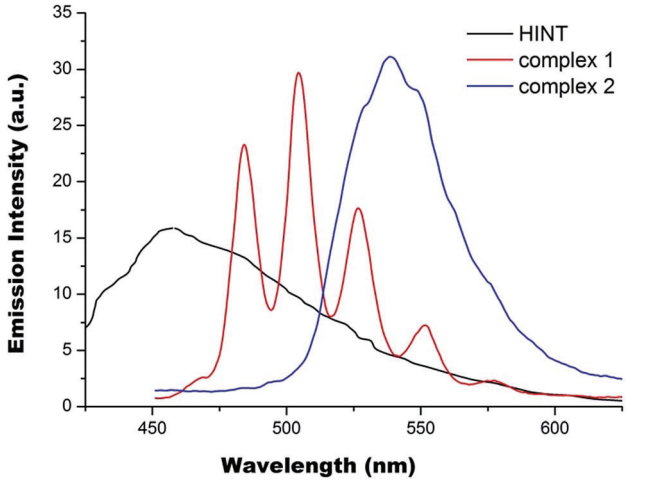

Fig. 4 The fluorescence emission spectra of **1**, **2** and HINT ligand.

U═O bond lengths of 1.788(7) Å and 1.778(5) Å,[19] respectively, consistent with the values determined by single crystal X-ray diffraction studies; bending vibrations of $(UO_2)^{2+}$ and $(U-O_{ligand})$ at 286 and 279 cm^{-1}; 2) the presence of INT in **1** and **2** including ν_{as} (COO^-) and ν_s (COO^-) at 1629–1524 cm^{-1} and 1403–1372 cm^{-1} for **1**, and 1525 cm^{-1} and 1409 cm^{-1} for **2**; carboxylate δ (COO^-) bending vibrations at 684, 467 and 235 cm^{-1} for **1**, and 686, 442 and 234 cm^{-1} for **2**.

Two outstanding differences between the two Raman spectra are also apparent. Firstly, the presence of nitrate anions in **1** is evident with the corresponding nitrate vibration modes at 1372, 1070 and 653 cm^{-1}.[20] Secondly, the presence of hydroxyl groups in **2** gives δ (U–O–H) bending vibrations at 1220 cm^{-1}. The detailed Raman assignments for the two complexes are summarized in Table S1.†

Photoluminescence

The fluorescence emission spectra for **1**, **2** and HINT ligand in fine powders were collected at ambient temperature using their maximum excitation wavelengths. The emission spectrum of HINT has a broad band with a maximum at around 455 nm, similar to the earlier observation.[21] The fluorescence emission spectrum of **1** (Fig. 4) has six emission bands at 470, 485, 505, 528, 555 and 579 nm, quite similar to that of uranyl nitrate hexahydrates with typical bands corresponding to the electronic transitions $S_{11} \rightarrow S_{00}$ and $S_{10} \rightarrow S_{0\nu}$ ($\nu = 0$–4) of the uranyl ion.[22] The most intense band is located at 505.0 nm (blue-shifted) for **1** compared to 510.0 nm observed for UNH.[22,23] The blue-shift effect is related to the presence of hexagonal bipyramidal uranium centres and has been discussed before.[24] The effect of INT in monodentate coordination mode has not been observed. The emission spectrum of **2** (Fig. 4) has a broad feature with the most intense band at 538 nm (red-shifted), together with shoulders at 530 and 553 nm. The slightly red-shift effect for some uranyl carboxylate compounds have been discussed and attributed to the presence of pentagonal bipyramidal uranium centres.[24] However, further red-shift and broad nature in the case of **2** could be the combined result of the uranium local coordination environment and the ligand effect *via* U–N bonding. All in all, the fluorescence emission spectrum of **1** is dominated by the presence of hexagonal bipyramidal uranium centre with no obvious ligand effect. However, the complexation of U(VI) ion by INT anions through μ_3-coordination mode *via* both bridging carboxylate group and U–N bonding has apparently enhanced fluorescence emission of **2** with significant red shift being witnessed. Note the fluorescence lifetimes for both compounds are fairly long, around 0.5 μs (Fig. S4†).

Conclusions

In summary, the reaction of uranyl nitrate and HINT at room temperature affords the formation of a monomeric complex **1** with both coordinated nitrate anions and HINT molecules in *trans*-positions. In addition, a new uranyl hydroxyl complex **2** with INT was synthesized under hydrothermal conditions. It has a 2D layered structure built with uranyl hydroxyl pillars linked through μ_3-bridging INT anions and is the first reported U(VI) compound with INT in μ_3-bridging mode *via* bridging carboxylate group and U–N bonding. The relatively higher final solution pH (~5.4) and consequently further hydrolysis of uranyl species are believed to be the reason favoring the formation of complex **2**. Thermal analysis confirmed both complexes lost organic ligand first, followed by further decomposition to form U_3O_8. Raman spectroscopy has been successfully used not only to confirm the presence of uranyl ion and INT anion in both complexes but also reveal the existence of nitrate vibrations in **1** and hydroxyl vibrations in **2**. Complex **1** has fluorescent emission spectrum similar to uranyl nitrate hexahydrates but slightly blue-shifted due to the presence of hexagonal bipyramidal uranium coordination environment. The significant red shift observed for **2** is thought to be due to the combined result of both pentagonal bipyramidal uranium local coordination environment and the ligand effect *via* both bridging carboxylate group and U–N bonding.

Acknowledgements

The crystallographic data collections were undertaken on the MX2 beamline at the Australian Synchrotron, Victoria, Australia.

References

1 (*a*) O. M. Yaghi, H. Li, C. Davis, D. Richardson and T. L. Groy, *Acc. Chem. Res.*, 1998, **31**, 474; (*b*) O. M. Yaghi, M. O'Keeffe, N. W. Ockwig, H. K. Chae, M. Eddaoudi and J. Kim, *Nature*, 2003, **423**, 705; (*c*) C. N. R. Rao, S. Natarajan and R. Vaidhyanathan, *Angew. Chem., Int. Ed.*, 2004, **43**, 1466; (*d*) M. D. Allendorf, C. A. Bauer, R. K. Bhakta and R. J. T. Houk, *Chem. Soc. Rev.*, 2009, **38**, 1330; (*e*) J. Y. Lee, O. K. Farha, J. Roberts, K. A. Scheidt, S. B. T. Nguyen and J. T. Hupp, *Chem. Soc. Rev.*, 2009, **38**, 1450.

2 (*a*) P. Thuéry, *Inorg. Chem. Commun.*, 2008, **11**, 616; (*b*) P. Thuéry, *CrystEngComm*, 2008, **10**, 79; (*c*) P. Thuéry, *CrystEngComm*, 2009, **11**, 1081; (*d*) P. Thuéry, *Cryst. Growth Des.*, 2011, **11**, 347; (*e*) J. Lhoste, N. Henry, P. Roussel, T. Loiseau and F. Abraham, *Dalton Trans.*, 2011, 2422; (*f*) I. Mihalcea, N. Henry and T. Loiseau, *Cryst. Growth Des.*, 2011, **11**, 1940; (*g*) I. Mihalcea, N. Henry, N. Clavier, N. Dacheux and T. Loiseau, *Inorg. Chem.*, 2011, **50**, 6243; (*h*) T. Loiseau, I. Mihalcea, N. Henry and C. Volkringer, *Coord. Chem. Rev.*, 2014, **266–267**, 69; (*i*) F. Abraham, B. Arab-Chapelet, M. Rivenet, C. Tamain and S. Grandjean, *Coord. Chem. Rev.*, 2014, **266–267**, 26.

3 P. Crançon and J. Van der Lee, *Radiochim. Acta*, 2003, **91**, 673.

4 M. B. Andrews and C. L. Cahill, *Chem. Rev.*, 2013, **113**, 1121.

5 E. V. Grechishnikova, Y. N. Mikhailov, A. S. Kanishcheva, L. B. Serezhkina and V. N. Serezhkin, *Russ. J. Inorg. Chem.*, 2005, **50**, 1436.

6 L. B. Serezhkina, A. V. Vologzhanina, S. A. Novikov, A. A. Korlyukov and V. N. Serezhkin, *Crystallogr. Rep.*, 2011, **56**, 258.

7 J.-Y. Kim, A. J. Norquist and D. O'Hare, *Chem. Mater.*, 2003, **15**, 1970.

8 D.-S. Liu, T.-Q. Shi, S.-F. Liu, S.-M. Ying and X.-F. Li, *Acta Crystallogr., Sect. E: Struct. Rep. Online*, 2007, **63**, m385.

9 (*a*) Y.-R. Xie, H. Zhao, X.-S. Wang, Z.-R. Qu, R.-G. Xiong, X. G. Xue, Z. Xue and X.-Z. You, *Eur. J. Inorg. Chem.*, 2003, 3712; (*b*) S. Lis, Z. Glatty, G. Meinrath and M. Kubicki, *J. Chem. Crystallogr.*, 2010, **40**, 646.

10 (*a*) E. V. Grechishnikova, E. V. Peresypkina, A. V. Virovets, Y. N. Mikhailov and L. B. Serezhkina, *Koord. Khim.*, 2007, **33**, 468; (*b*) V. I. Mishkevich, M. S. Grigoriev, A. M. Fedosseev and P. Moisy, *Acta Crystallogr., Sect. E: Struct. Rep. Online*, 2012, **68**, m1243; (*c*) W. Aas and M. H. Johansson, *Acta Chem. Scand.*, 1999, **53**, 581; (*d*) P. R. Silverwood, D. Collison, F. R. Livens, R. L. Beddoes and R. J. Taylor, *J. Alloys Compd.*, 1998, **271**, 180; (*e*) P. Thuéry, *Inorg. Chem. Commun.*, 2009, **12**, 800; (*f*) R. C. Severance, S. A. Vaughn, M. D. Smith and H.-C. Zur Loye, *Solid State Sci.*, 2011, **13**, 1344.

11 M. B. Andrews and C. L. Cahill, *CrystEngComm*, 2011, **13**, 7068.

12 T. M. McPhillips, S. E. McPhillips, H. J. Chiu, A. E. Cohen, A. M. Deacon, P. J. Ellis, E. Garman, A. Gonzalez, N. K. Sauter, R. P. Phizackerley, S. M. Soltis and P. Kuhn, *J. Synchrotron Radiat.*, 2002, **9**, 401.

13 W. Kabsch, *J. Appl. Crystallogr.*, 1993, **26**, 795.

14 G. M. Sheldrick, *Acta Crystallogr., Sect. A: Found. Crystallogr.*, 2008, **64**, 112.

15 S. Kannan, S. B. Deb, J. S. Gamare and M. G. B. Drew, *Polyhedron*, 2008, **27**, 2557.

16 E. V. Mit'kovskaya, Y. N. Mikhailov, Y. E. Gorbunova, L. B. Serezhkina and V. N. Serezhkin, *Russ. J. Inorg. Chem.*, 2004, **49**, 1538.

17 N. A. Budantseva, G. B. Andreev, A. M. Fedoseev, M. Yu. Antipin and J.-C. Krupa, *Radiochim. Acta*, 2006, **94**, 69.

18 (*a*) P. C. Debets, *Acta Crystallogr.*, 1966, **21**, 589; (*b*) E. Gómez-Rebollo, P. Herrero and R. M. Rojas, *J. Nucl. Mater.*, 1997, **245**, 161; (*c*) J. Čejka, J. Sejkora, Z. Mrázek, Z. Urbanec and T. Jarchovský, *Neues Jahrbuch für Mineralogie Abhandlungen*, 1996, **170**, 155; (*d*) K. Sudo and A. Okawa, *Bull. Res. Inst. Miner. Dressing Metall., Tohoku Univ.*, 1960, **16**(1), 85.

19 J. R. Bartlett and R. P. Cooney, *J. Mol. Struct.*, 1989, **193**, 295.

20 L. M. Toth and G. M. Begun, *J. Phys. Chem.*, 1981, **85**(5).

21 W.-T. Chen, *Bull. Chem. Soc. Ethiop.*, 2011, **25**(2), 233.

22 (*a*) C. Jacopin, M. Sawicki, G. Plancque, D. Dozi, F. Taran, E. Ansoborlo, B. Amekraz and C. Moulin, *Inorg. Chem.*, 2003, **42**, 5015; (*b*) A. F. Leung, L. Hayashibara and J. Spadaro, *J. Phys. Chem. Solids*, 1999, **60**, 429.

23 (*a*) Y.-N. Hou, Y.-H. Xing, F.-Y. Bai, Q.-L. Guan, X. Wang, R. Zhang and Z. Shi, *Spectrochim. Acta, Part A*, 2014, **123**, 267; (*b*) Y. Zhang, M. Bhadbhade, I. Karatchevtseva, J. R. Price, H. Liu, Z. Zhang, L. Kong, J. Čejka, K. Lu and G. R. Lumpkin, *J. Solid State Chem.*, 2015, **226**, 42.

24 (*a*) I. Mihalcea, N. Henry, C. Volkringer and T. Loiseau, *Cryst. Growth Des.*, 2012, **12**, 526; (*b*) T. Loiseau, I. Mihalcea, N. Henry and C. Volkringer, *Coord. Chem. Rev.*, 2013, **266–267**, 69; (*c*) I. Mihalcea, N. Henry and T. Loiseau, *Eur. J. Inorg. Chem.*, 2014, 1322.